The Plant Journal (2005) **41**, 412–428 doi: 10.1111/j.1365-313X.2004.02307.x

In vivo studies on the roles of Tic110, Tic40 and Hsp93 during chloroplast protein import

Sabina Kovacheva[1,†], Jocelyn Bédard[1,†], Ramesh Patel[1], Penny Dudley[1], David Twell[1], Gabino Ríos[2], Csaba Koncz[2] and Paul Jarvis[1,*]

[1]*Department of Biology, University of Leicester, Leicester LE1 7RH, UK, and*

[2]*Max-Planck Institut für Züchtungsforschung, Carl-von-Linné-Weg 10, D-50829 Köln, Germany*

Received 25 October 2004; accepted 4 November 2004.

[*]For correspondence (fax +44 116 252 3330; e-mail rpj3@le.ac.uk).

[†]These authors contributed equally to this work.

Summary

A multisubunit translocon of the inner envelope membrane, termed Tic, mediates the late stages of protein import into chloroplasts. Membrane proteins, Tic110 and Tic40, and a stromal chaperone, Hsp93, have been proposed to function together within the Tic complex. In Arabidopsis, single genes, *atTIC110* and *atTIC40*, encode the Tic proteins, and two homologous genes, *atHSP93-V* and *atHSP93-III*, encode Hsp93. These four genes exhibited relatively uniform patterns of expression, suggesting important roles for plastid biogenesis throughout development and in all tissues. To investigate the roles played by these proteins *in vivo*, we conducted a comparative study of T-DNA knockout mutants for each Tic gene, and for the most abundantly expressed Hsp93 gene, *atHSP93-V*. In the homozygous state, the *tic110* mutation caused embryo lethality, implying an essential role for atTic110 during plastid biogenesis. Homozygous *tic110* embryos exhibited retarded growth, developmental arrest at the globular stage and a 'raspberry-like' embryo-proper phenotype. Heterozygous *tic110* plants, and plants homozygous for the *tic40* and *hsp93-V* mutations, exhibited chlorosis, aberrant chloroplast biogenesis, and inefficient chloroplast-import of both photosynthetic and non-photosynthetic preproteins. Non-additive interactions amongst the mutations occurred in double mutants, suggesting that the three components may cooperate during chloroplast protein import.

Keywords: Arabidopsis, chloroplast protein import, protein targeting, Tic110, Tic40, Hsp93.

Introduction

Chloroplast biogenesis is dependent on >90% nucleus-encoded proteins, which are imported into the organelle in an energy-dependent and post-translational manner from the cytosol. The passage of proteins through the double envelope membrane is mediated by the coordinate action of membrane-bound proteins and soluble factors (Jackson-Constan *et al.*, 2001; Jarvis and Soll, 2002; Schnell and Hebert, 2003). The membrane-bound proteins form two heteroligomeric complexes, termed Toc and Tic (for Translocon at the outer/inner envelope membrane of chloroplasts). The Toc complex has been studied most extensively, and biochemical studies using pea chloroplasts have resulted in the identification of several Toc components. Two GTPases, Toc159 and Toc34, control preprotein recognition (Hirsch *et al.*, 1994; Kessler *et al.*, 1994; Perry and Keegstra, 1994; Schnell *et al.*, 1994; Seedorf *et al.*, 1995), and Toc75, a beta-barrel protein, constitutes at least part of the translocation channel (Hinnah *et al.*, 1997; Schnell *et al.*, 1994; Tranel *et al.*, 1995).

Several components of the Tic complex have also been identified, but their functions are less well characterized than those of the Toc components. Tic110 was the first to be identified, and it is a major component of Tic complexes (Kessler and Blobel, 1996; Kouranov *et al.*, 1998; Lübeck *et al.*, 1996; Schnell *et al.*, 1994; Wu *et al.*, 1994). It has two N-terminal transmembrane domains and a large (approximately 98 kDa) C-terminal hydrophilic domain which is exposed on the stromal side of the membrane (Inaba *et al.*, 2003; Jackson *et al.*, 1998; Kessler and Blobel, 1996). The function of Tic110 is still debated, but it has been proposed to play roles in the formation of the inner envelope translocation channel (Heins *et al.*, 2002), and the recruitment of molecular chaperones to the stromal face of the Tic complex (Akita *et al.*, 1997; Kessler and Blobel, 1996; Nielsen *et al.*,

1997). In support of the latter hypothesis, co-immunoprecipitation and cross-linking experiments revealed that Tic110 is in close proximity to the stromal Hsp100 chaperone, Hsp93, as well as another membrane protein, Tic40 (Akita *et al.*, 1997; Chou *et al.*, 2003; Nielsen *et al.*, 1997; Stahl *et al.*, 1999). A recent study on the structure, topology and behaviour of *Arabidopsis thaliana* Tic110 (atTic110) also supports the latter model (Inaba *et al.*, 2003). Direct interaction between atTic110 and preproteins was demonstrated, suggesting that the stromal bulk of the protein serves also as a docking site for preproteins as they emerge from the Tic translocon. Thus, Tic110 may function as a scaffold for coordinating the stromal events of protein import into chloroplasts (Inaba *et al.*, 2003).

Tic40 has been found associated with preproteins arrested during protein import (Wu *et al.*, 1994), and in cross-linked complexes containing Tic110 and Hsp93 (Chou *et al.*, 2003; Stahl *et al.*, 1999). It has a single N-terminal transmembrane domain, and the bulk of the protein projects into the stroma (Chou *et al.*, 2003; Stahl *et al.*, 1999). While T-DNA knockout mutants have confirmed that the protein plays a role in chloroplast protein import (Chou *et al.*, 2003), the precise nature of this role remains unclear (Ko *et al.*, 2004). Interestingly, its function has been assigned to a stage of import during which Tic110 and Hsp93 also operate (Chou *et al.*, 2003). Tertiary structure prediction and immunological studies have indicated that a central portion of Tic40 contains a putative tetratricopeptide repeat (TPR) protein–protein interaction domain (Chou *et al.*, 2003). This TPR domain is followed by a C-terminal domain with sequence homology to mammalian co-chaperones – Hsp70-interacting protein (Hip) and Hsp70/Hsp90-organizing protein (Hop) (Frydman and Höhfeld, 1997; Höhfeld *et al.*, 1995) – which themselves contain TPR-domains. Thus, Tic40 most likely plays a co-chaperone role during chloroplast protein import.

Hsp93 proteins are stromal chaperones that belong to the caseinolytic protease (Clp) C class of the Hsp100 chaperones, and have been identified in several plant species including Arabidopsis (Moore and Keegstra, 1993; Shanklin *et al.*, 1995; Zheng *et al.*, 2002). ClpC chaperones have two highly conserved Walker-type nucleotide-binding motifs, a spacer of intermediate length and two conserved N-terminal domains (Schirmer *et al.*, 1996). They play roles in protein folding and disaggregation and, when in association with the ClpP protease, they act to target proteins for degradation by ClpP. However, their functions in plants have not yet been precisely defined. Shanklin *et al.* (1995) demonstrated that pea Hsp93 is able to functionally substitute for *Escherichia coli* ClpA in an *in vitro* ClpP proteolysis assay, and a possible association between spinach Hsp93 and chloroplastic ClpP proteases was revealed by Sokolenko *et al.* (1998). In addition, because of their association with the Tic complex, these chaperones have also been proposed to provide the driving force for chloroplast protein import (Akita *et al.*, 1997; Nielsen *et al.*, 1997). This is an attractive hypothesis because it is well documented that chaperones provide the driving force for protein import into mitochondria and the endoplasmic reticulum (Matlack *et al.*, 1999; Neupert and Brunner, 2002). In these systems, the important chaperones (mtHsp70 and BiP respectively) are both members of the Hsp70 family. Interestingly, although Hsp70 proteins are present in the chloroplast stroma, stable associations between Tic110 and Hsp70 have not been detected (Nielsen *et al.*, 1997). ClpC chaperones might employ a similar mechanism during chloroplast protein import to that which they use during the translocation of degradation substrates into the ClpP complex.

In light of these various data, it is tempting to speculate that Tic110, Tic40 and Hsp93 function together to provide the driving force for preprotein translocation. The paradigm for this hypothesis is provided by the mitochondrial protein import motor. This motor is composed of two membrane proteins, Tim44 and Tim14, and two matrix proteins, mtHsp70 and Mge1 (Mokranjac *et al.*, 2003; Neupert and Brunner, 2002; Pfanner *et al.*, 1997). Tim44 is anchored in the inner mitochondrial membrane and projects a large domain into the matrix. It functions to recruit mtHsp70 to the inner surface of the Tim complex, which then binds to translocating preproteins as they emerge from the channel, preventing retrograde movement and perhaps even imparting inward 'pulling' force (Neupert and Brunner, 2002). Successive rounds of ATP hydrolysis by mtHsp70 – stimulated by two co-chaperones: the J-domain protein, Tim14, and the nucleotide-exchange factor, Mge1 – ultimately lead to the complete translocation of the preprotein into the matrix (Mokranjac *et al.*, 2003; Neupert and Brunner, 2002; Pfanner *et al.*, 1997). During chloroplast protein import, Tic110, Tic40 and Hsp93 might play roles analogous to those played by Tim44, Tim14/Mge1 and mtHsp70 respectively.

As described above, current evidence for the cooperation of Tic110, Tic40 and Hsp93 during chloroplast protein import is tentative, and based largely on biochemical data. To address the functional relationships between these three proteins in an *in vivo* context, we conducted a comparative study of Arabidopsis T-DNA knockout mutants lacking each component. Data derived from such genetic studies are complementary to those obtained using biochemical approaches (Bauer *et al.*, 2000; Chen *et al.*, 2002; Gutensohn *et al.*, 2000; Jarvis *et al.*, 1998; Kubis *et al.*, 2003).

Results

Expression profiles of Arabidopsis Tic110, Tic40 and Hsp93 genes

In Arabidopsis, Tic110 and Tic40 are each encoded by a single gene, *atTIC110* and *atTIC40*, whereas Hsp93 is encoded by

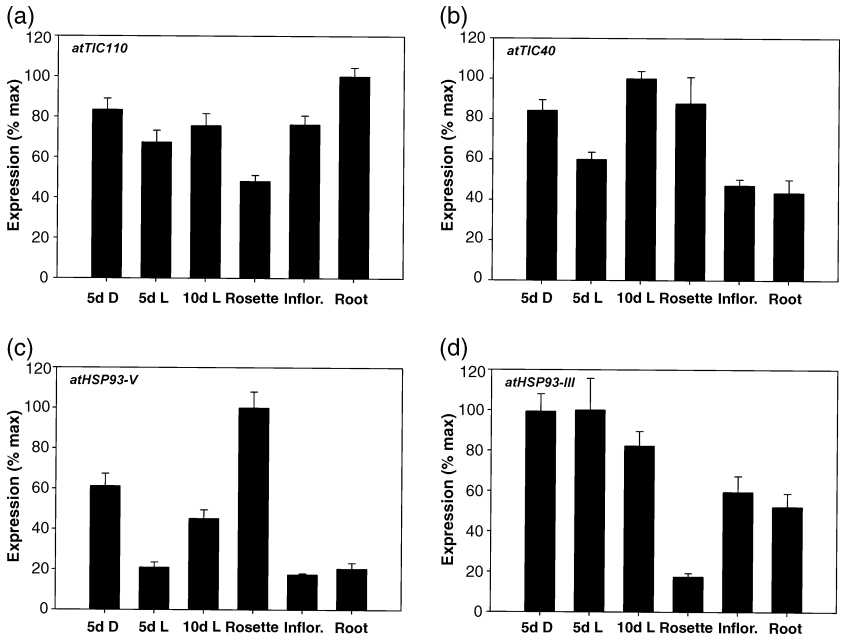

Figure 1. Expression profiles of the *atTIC110*, *atTIC40*, *atHSP93-V* and *atHSP93-III* genes.
Total RNA samples isolated from wild type were analysed by RT-PCR using *atTIC110* (a), *atTIC40* (b), *atHSP93-V* (c) and *atHSP93-III* (d) gene-specific primers. RNA was isolated from whole seedlings grown *in vitro* for 5 days in the dark (5d D), or 5 and 10 days in the light (5d L and 10d L respectively), or from three different tissues of 28-day-old plants gown on soil (rosette leaves, inflorescences and roots). RNA samples were representative of approximately 200–300 seedlings (5d D, 5d L and 10d L), or five to 25 mature plants (rosettes, inflorescences and roots). Amplifications were conducted using non-saturating conditions, and PCR products were quantified by hybridization with [^{32}P]-labelled, gene-specific probes. Values shown are means derived from four PCR amplifications (±SD), and are expressed as a percentage of the maximum value obtained for each gene. The data were normalized using similarly derived data for the gene encoding translation initiation factor eIF4E1.

two different genes, *atHSP93-V* and *atHSP93-III* (Jackson-Constan and Keegstra, 2001). The proteins encoded by these Arabidopsis genes are highly similar to the proteins originally identified in pea (Kessler and Blobel, 1996; Lübeck *et al.*, 1996; Moore and Keegstra, 1993; Stahl *et al.*, 1999): amino acid sequence identities shared between the mature forms of the proteins are 67% (atTic110), 56% (atTic40), 92% (atHsp93-V) and 87% (atHsp93-III). The two Arabidopsis Hsp93 proteins share 91% sequence identity. To gain an initial insight into the functional relationships between the Tic proteins and the Hsp93 chaperones in Arabidopsis, we examined their developmental and tissue-specific gene expression patterns by semi-quantitative RT-PCR.

The data revealed that expression of the *atTIC110*, *atTIC40*, *atHSP93-V* and *atHSP93-III* genes occurs throughout development, and is not restricted to photosynthetic or non-photosynthetic tissues (Figure 1). Expression levels of *atTIC110* and *atTIC40* during periods of intense growth in young tissues were comparable with those observed during maturation in older tissues: compare expression levels in 5- or 10-day-old plants with those in rosette leaves (Figure 1a,b). The Hsp93 homologues exhibited slightly more regulated expression patterns than the Tic genes: expression of *atHSP93-V* reached a maximum in rosette leaves (Figure 1c), whereas *atHSP93-III* expression was reduced in the same tissue (Figure 1d). These moderately regulated and complementary expression patterns may reflect functional redundancy between atHsp93-V and atHsp93-III, suggesting that declining expression of one homologue is compensated for by increased expression of the other. On the other hand, *atHSP93-V* is expressed at significantly higher levels than *atHSP93-III*. Five fewer PCR cycles were required to amplify the same amount of *atHSP93-V* cDNA, and there are three times more expressed sequence tags for *atHSP93-V* in the databases. Furthermore, when the expression levels of the two genes in 12-day-old plants were compared by RNA gel blot analysis using gene-specific probes of identical specific activity, the signal intensity observed for *atHSP93-V* was approximately 15-fold higher than that observed for *atHSP93-III* (Supplementary Figure S1). This result is broadly in agreement with the RT-PCR data of Zheng *et al.* (2002): these authors observed a stronger signal for *atHSP93-V* (*clpC1*) than for *atHSP93-III* (*clpC2*), even though fivefold more template was used in the *atHSP93-III* amplifications.

Overall, however, it appears that all four genes are expressed at significant levels throughout development. These expression data are therefore consistent with the proposed roles of the proteins as general components of the import machinery, and with the possibility that the proteins function together during chloroplast protein import. Relatively high levels of expression of all four genes were observed in etiolated seedlings (Figure 1), which may indicate an important role for the proteins even during very early stages of plastid development.

Identification of tic110, tic40 *and* hsp93-V *knockout mutants*

To investigate the roles of the three proteins in an *in vivo* context, we isolated Arabidopsis knockout mutants for atTic110, atTic40 and atHsp93-V, the most abundantly expressed Hsp93 isoform, and conducted a comprehensive comparative study of the mutant phenotypes. The mutants were isolated by screening various populations of

transferred DNA (T-DNA) mutagenized plants, either *in silico* or by PCR using gene-specific and T-DNA primers. Figure 2(a) shows schematic representations of the three genes, including the location of each T-DNA insertion. In parallel with us, another group independently isolated atTic40 knockout mutants (Chou *et al.*, 2003). The results of Chou *et al.* (2003) are therefore discussed extensively throughout this report.

We identified two, independent alleles of each knockout mutation. Initially, we identified two alleles of *tic40* (*tic40-3* and *tic40-4*) and one allele each of the other mutations (*tic110-1* and *hsp93-V-1*). All of the data presented in this report (unless specifically indicated otherwise) were derived using these original lines; the two *tic40* alleles were used interchangeably and gave identical results. The additional *tic110* and *hsp93-V* alleles shown in Figure 2(a) were identified subsequently, and were used to confirm results obtained using the original alleles; data derived using these additional alleles are referred to specifically in the relevant sections below.

In segregating families, the selectable markers associated with the *tic40* and *hsp93-V* T-DNA insertions all showed standard Mendelian inheritance (3:1 segregation ratios), indicating the presence of a single T-DNA insertion site in

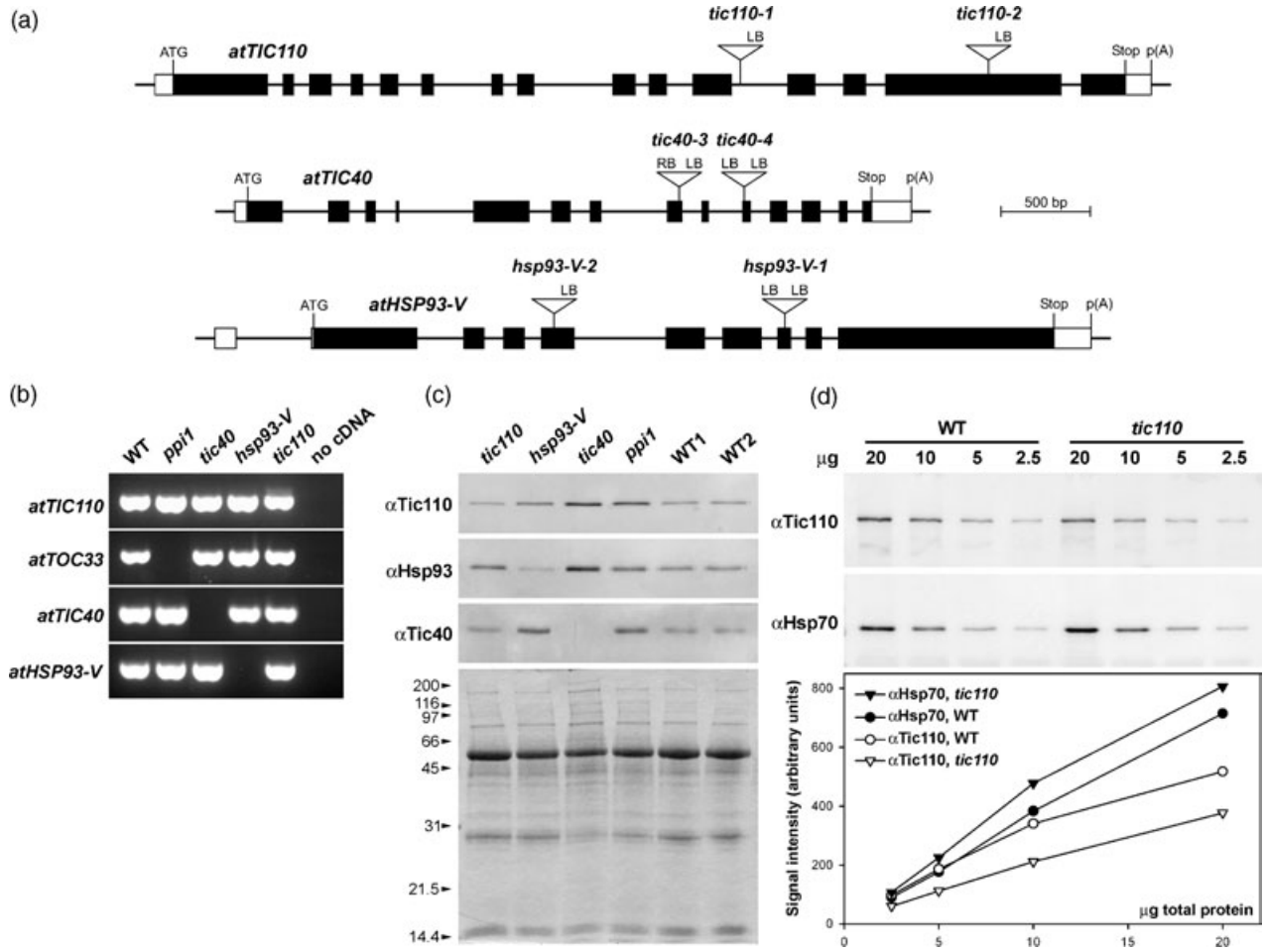

Figure 2. Knockout mutations affecting the *atTIC110*, *atTIC40* and *atHSP93-V* genes.
(a) Schematics showing the structure of each gene and the location of each T-DNA insertion. Protein-coding exons are represented by black boxes, and untranslated regions by white boxes; introns are represented by thin lines between the boxes. T-DNA insertion sites are indicated precisely, but the insertion sizes are not to scale. ATG, translation initiation codon; Stop, translation termination codon; p(A), polyadenylation site; LB, T-DNA left border; RB, T-DNA right border.
(b) RT-PCR analysis of the expression of the *atTIC110*, *atTIC40* and *atHSP93-V* genes in 10-day-old plants grown *in vitro*. Amplification was conducted using gene-specific primers (indicated at left), and the products were visualized by staining with ethidium bromide following agarose gel electrophoresis. The template included in each PCR reaction is indicated at the top. The *atTOC33* gene and the *ppi1* mutant were included in this experiment as controls.
(c) Immunoblot analysis of the expression of the atTic110, atTic40 and atHsp93 proteins in 14-day-old plants. Total chloroplast protein samples (10 μg each) isolated from the genotypes indicated at the top were separated by SDS-PAGE and transferred to nitrocellulose membranes. Filters were probed with antibodies against Tic110, Tic40 and Hsp93, as indicated. The lower panel shows an identical SDS-PAGE gel stained with Coomassie brilliant blue as a loading control. The *ppi1* mutant was included as a control.
(d) Immunoblot analysis of atTic110 protein in the *tic110* mutant. Dilution series of total protein samples isolated from the sixth true leaf of 19-day-old wild-type and *tic110* mutant plants were analysed using antibodies against Tic110 and, as a control, stromal Hsp70; the amount of protein loaded in each lane is indicated in micrograms. All bands were quantified using Quantity One software (Bio-Rad), and then plotted against the amount of total protein loaded in each case.

Table 1 Genetic analyses of the *tic110*, *tic40* and *hsp93-V* mutants

Genotype	Generation	Selection	Resistant (if plated on selection)			Sensitive	Green:pale	Resistant:sensitive	χ^2-value[e]	*P*-value[e]
			Green	Pale	Total resistant					
tic110-1	T_3	None	197	296[a]	–	–	1.00:1.50	–	9.74	1.80×10^{-3}
		Phosphinothricin	476[b]	–	476[b]	312	–	1.53:1.00	13.90	1.93×10^{-4}
tic40-3	F_2^c	None	290	102	–	–	2.84:1.00	–	0.22	0.64
	F_3^c	Hygromycin	418	215	633	237	–	2.67:1.00	2.33	0.13
tic40-4	T_3	None	612	195	–	–	3.14:1.00	–	0.30	0.58
		Phosphinothricin	537	254	791	287	–	2.76:1.00	1.52	0.22
hsp93-V-1	T_3	None	307	111	–	–	2.77:1.00	–	0.54	0.46
		Phosphinothricin	298	109	407	125	–	3.26:1.00	0.64	0.42
tic110-2	T_4	None	298	489[a]	–	–	1.00:1.64	–	7.27	7.00×10^{-3}
		Kanamycin	297[b]	–	297[b]	180	–	1.65:1.00	4.16	4.14×10^{-2}
hsp93-V-2	T_4	None	487	157	–	–	3.10:1.00	–	0.13	0.72
		Kanamycin	250[d]	–	250[d]	74	–	3.38:1.00	0.81	0.37

[a]The pale/yellow-green phenotypes of *tic110-1* and *tic110-2* were scored after 21 days growth on soil.
[b]All seedlings were classified as green due to the lack of a clear pale/yellow-green phenotype in young, *in vitro*-grown *tic110* plants.
[c]These plants were derived from a back-cross to Col-0 wild type.
[d]All seedlings were classified as green due to scoring difficulties caused by the genetic silencing of the kanamycin resistance marker.
[e]Chi-square tests evaluated 'goodness of fit' of the observed ratios to 3:1 (*tic40* and *hsp93-V*) and 2:1 (*tic110*) respectively; degrees of freedom = 1.

each case (Table 1). By contrast, both *tic110* T-DNA insertions produced segregation ratios of approximately 2:1, suggesting that the *tic110* mutation may be lethal, in the homozygous state, during a very early stage of development (Table 1). Accordingly, when 22 plants carrying the *tic110-1* T-DNA insertion (selected based on their phosphinothricin resistance) were genotyped by PCR, all were found to be heterozygous for the mutation (data not shown). Therefore, all analyses of the *tic110* mutants were conducted using heterozygous plants. For the other mutants (*tic40* and *hsp93-V*), homozygous lines were identified phenotypically based on the T-DNA-associated selectable marker, and by PCR analysis.

To confirm that each of the mutants is null for the respective component, we employed RT-PCR and immunoblotting (Figure 2b,c). The RNA (for RT-PCR) and isolated chloroplast (for immunoblotting) samples used for these experiments were derived from 10- and 14-day-old homozygous individuals grown *in vitro* respectively; in the case of the *tic110* mutant, heterozygous individuals were used. The atToc33 knockout mutant, *ppi1*, was included as a control in each experiment (Jarvis *et al.*, 1998). Figure 2(b) demonstrates that each T-DNA insertion (with the exception of the *tic110* insertion) abolishes expression of the corresponding full-length mRNA; the *tic110* mutant displayed residual *atTIC110* expression because the plants were not homozygous for the T-DNA insertion. Figure 2(c) shows that all three proteins are present in isolated chloroplasts, confirming their localization in this organelle. Furthermore, all of the mutants were found to be at least partly deficient in the appropriate component (Figure 2c). However, only *tic40* was found to completely lack the relevant protein. The fact that Hsp93 protein could be detected in the *hsp93-V* mutant most likely indicates that the anti-pea-Hsp93 polyclonal antibody used does not distinguish between the two Arabidopsis Hsp93 proteins, which share 91% sequence identity; the fact that *hsp93-V* is null at the mRNA level (Figure 2b) supports this conclusion.

The data presented in Figure 2(b,c) suggested that Tic110 expression is slightly reduced in *tic110* heterozygotes. To obtain more conclusive evidence for this apparent gene-dosage effect, we analysed atTic110 protein abundance in young leaves of more mature plants (the visible phenotype associated with the heterozygous *tic110* mutation is more pronounced during later development; see later). Dilution series of wild-type and mutant protein samples were used to prepare blots, and these were probed for Tic110 and, as a control, stromal Hsp70 (Figure 2d). When the Tic110 bands were quantified and normalized with respect to Hsp70, we were able to deduce that Tic110 protein abundance in *tic110* heterozygotes is equivalent to approximately 49.5% ($\pm$2.1%; $n = 3$) of the wild-type level; signal intensities were found to saturate slightly at the highest protein concentration (20 μg; Figure 2d), and so only data for the three lowest protein concentrations (2.5, 5 and 10 μg) were used in our calculations. These data confirm that *tic110* affects the accumulation of atTic110 protein, even in the heterozygous state.

The tic110 *mutation is embryo-lethal*

The non-Mendelian segregation ratios associated with both *tic110* T-DNA insertions (Table 1), and the fact that all

22 phosphinothricin-resistant *tic110-1* plants that we genotyped by PCR were heterozygous for the mutation (data not shown), suggested that the homozygous *tic110* genotype may be lethal during embryogenesis. To investigate this possibility, we analysed the seeds within seven mature *tic110-1* siliques and 30 mature *tic110-2* siliques. As expected, aborted seeds were observed at a relatively high frequency in each of the *tic110* siliques examined (Figure 3a). We observed 101 aborted seeds in a total of 387 seeds in the *tic110-1* mutant, and 397 aborted seeds in a total of 1544 in the *tic110-2* mutant. The frequency of the aborted seeds (approximately 25% in each case) strongly suggests that *tic110* is embryo-lethal in the homozygous state. The fact that the marker genes associated with both *tic110* T-DNA insertions segregated with ratios slightly less than 2:1 (Table 1) suggests that the mutation may also have a slight effect on gametophytic transmission.

To determine the stage of development at which *tic110* exerts its embryo-lethal effect, we characterized embryogenesis in *tic110* mutant plants using Nomarski optics. Figure 3 shows equivalent developmental series for normal (panels b–e) and mutant (panels f–i) embryos within immature, heterozygous *tic110* siliques. Morphologically, normal and mutant embryos were almost indistinguishable at the proembryo stage in young *tic110* siliques (data not shown), and stereotypic cell division patterns were observed within the embryo-proper and suspensor regions of most embryos (data not shown). However, early defects do occur in *tic110* homozygotes, because abnormal, asymmetric (Figure 3f) or unsynchronized (Figure 3g) divisions were observed in some delayed embryos within older siliques that contained either globular- or triangular-stage normal embryos (Figure 3, compare b with f, and c with g).

Mutant embryos displayed retarded development, such that the embryos within *tic110* siliques spanned more than two developmental stages (Table 2, mutant siliques 3–9); embryos within wild-type siliques span only two successive stages (Table 2). The proportion of embryos showing delayed development in *tic110* siliques could most easily be determined when the majority of normal embryos within those siliques were at the torpedo stage (Figure 3e). In mutant siliques 7–9, for example, 20–24% of embryos were delayed at the proembryo or globular stages (Table 2). Although mutant embryos did reach the procambial stage, clear protuberances appeared on the surface of the embryo-proper, giving these embryos an abnormal, 'raspberry-like' phenotype (Figure 3i) (Apuya *et al.*, 2002; Yadegari *et al.*, 1994). Suspensor formation was essentially normal in *tic110* homozygotes, although we did observe further division of the uppermost suspensor cell (the hypophysis), which normally contributes to the root cap (Figure 3h,i).

Mutant embryos did not progress beyond the globular stage, and the endosperm remained uncellularized in mutant seeds (Figure 3i). Accumulation of chlorophyll (which normally commences at the heart stage when chloroplast development initiates) was never observed within mutant *tic110* embryos (data not shown). In conclusion, our data indicate that functional atTic110 protein is essential for embryo development and morphogenesis beyond the globular stage.

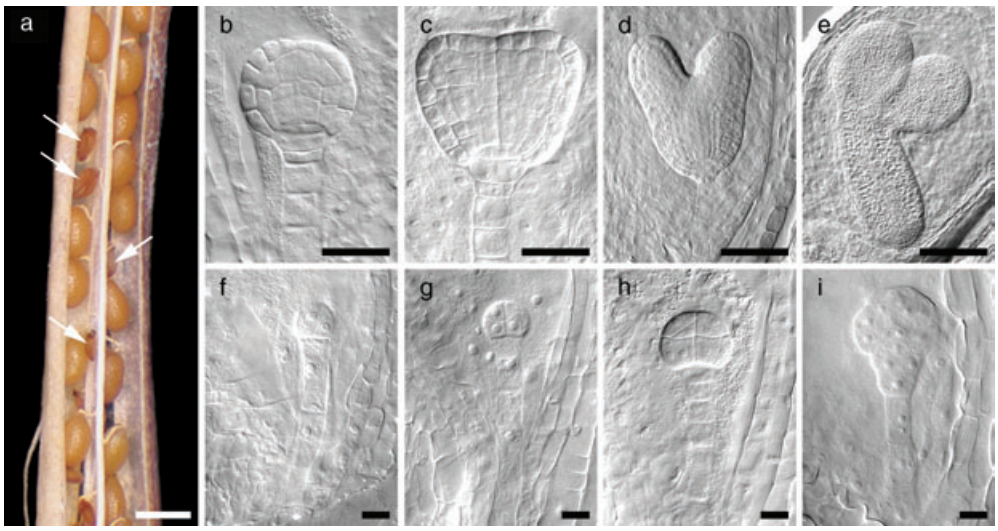

Figure 3. Phenotypic analyses of *tic110* embryo development.
(a) A typical, mature silique of a heterozygous *tic110* plant, containing both normal and aborted seeds. Aborted seeds (four of which are indicated with arrows) occur at a frequency of approximately 25% in *tic110* siliques. Bar represents 0.5 mm.
(b–i) Normal (b–e) and *tic110* mutant (f–i) embryos at different developmental stages within *tic110* heterozygous siliques. Normal embryos: (b) globular stage, (c) triangular stage, (d) heart stage, (e) torpedo stage. Corresponding mutant embryos from the same siliques: (f) four-cell stage, (g) eight-cell stage, (h) 32-cell stage, (i) globular, 'raspberry-like' stage. Embryo stage names refer to the number of cells in the embryo-proper, or the morphology of the embryo-proper. Bars represent 25 μm (b, c), 50 μm (d), 100 μm (e) or 10 μm in (f–i).

Table 2 Distribution of embryo phenotypes in single siliques of wild-type and *tic110* heterozygous plants

Silique	Proembryo[a]	Globular	Heart	Torpedo	Cotyledon
WT (Col-0)					
1	68				
2	57				
3	45	20			
4	10	48			
5		33	37		
6		3	70		
7			46	21	
8				5	68
9				2	64
Mutant (+/*tic110*)					
1	53				
2	18	8			
3	17	14	4		
4	14	8	18		
5	10	9	31		
6	14	4	26		
7	10		13	21	
8	5	5	12	27	
9		12		21	18

[a]Proembryo stage includes one-cell to 16-cell stage embryos. Embryo developmental stage names refer to the morphology of the embryo-proper.

The knockout mutants have chlorotic phenotypes

The visible phenotypes of the mutants were examined under *in vitro* growth conditions, and also when the plants were grown on soil. We observed that all of the knockout mutants displayed visible, yellow-green phenotypes (Figure 4a, Table 1), providing evidence for the involvement of each protein in chloroplast biogenesis. The *tic40-3* and *tic40-4* mutants described here (both Col-0 ecotype) appeared very similar to the *tic40-2* mutant (also Col-0 ecotype) described by Chou *et al.* (2003), but not as severely pale as the *tic40-1* mutant (Ws ecotype). Such ecotypic effects on mutant phenotype severity have been suggested previously (Ivanova *et al.*, 2004; Kubis *et al.*, 2004).

Amongst the different mutants reported here, *tic40* exhibited the most severely chlorotic phenotype, *hsp93-V* had an intermediate phenotype and heterozygous *tic110* plants had the weakest phenotype. It is particularly interesting that heterozygous *tic110* plants have a chlorotic phenotype (indicating that the *tic110* mutation is semi-dominant), as the *tic40* and *hsp93-V* mutations are completely recessive (Table 1), as indeed are other, previously described import apparatus mutations (Bauer *et al.*, 2000; Jarvis *et al.*, 1998). The *tic40* and *hsp93-V* mutants were significantly smaller than the wild type (Figure 4a), but nevertheless flowered at about the same time as wild-type plants (data not shown). All of the mutants were able to complete their life cycle and produce seeds.

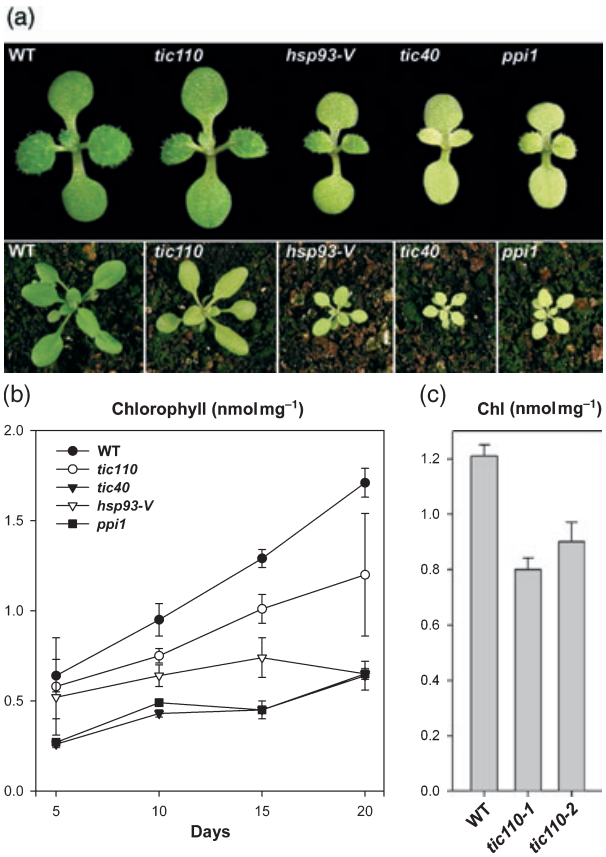

Figure 4. The knockout mutants have chlorotic phenotypes.
(a) The visible phenotypes of the *tic110*, *tic40* and *hsp93-V* mutants after 10 days growth *in vitro* (upper panel) or 24 days growth on soil (lower panel). The *ppi1* mutant is included as a control in each case.
(b) Chlorophyll accumulation in the mutants was quantified over a developmental time course. Leaf tissue was harvested from plants grown on soil in a greenhouse at 5-day intervals, starting on the fifth day after germination, and the chlorophyll levels were determined photometrically. Values shown are mean ± SD derived from four replicates, and indicate the amount of chlorophyll per mg fresh weight of tissue.
(c) Chlorophyll concentrations in heterozygotes carrying the two independent *tic110* alleles were quantified. Leaf tissue was harvested from plants grown on soil in a growth cabinet after 20 days growth, and the chlorophyll levels were determined photometrically. Values shown are means (± SD) derived from five replicates, and indicate the amount of chlorophyll per mg fresh weight of tissue.

To quantify the severity of chlorosis in the knockout mutants, we made chlorophyll measurements. Developmental fluctuations in chlorophyll accumulation were assessed by conducting a time-course analysis, starting on the fifth day after germination. All mutant plants contained reduced chlorophyll concentrations throughout development, regardless of whether they were grown *in vitro* (data not shown) or on soil (Figure 4b). Although only moderate chlorophyll deficiencies were found in the *tic110* mutant, this phenotype was clearly apparent in heterozygotes of both *tic110* alleles (Figure 4c). The mutant with the most severe visible phenotype, *tic40*, also displayed the lowest

pigment concentrations, reaching only one-third of the wild-type level by the end of the analysis. This mutant behaved much like *ppi1*, which was included again for comparison (Figure 4b). The chlorophyll content of *hsp93-V* plants increased until the 15th day (Figure 4b), after which a slight reduction in chlorophyll concentration occurred. This observation may reflect the fact that *atHSP93-V* is expressed at particularly high levels during later development (Figure 1c). Alternatively, it may indicate that an additional role for atHsp93-V (e.g. proteolysis) comes into play later in development.

In summary, the data indicate that all three genes are important for chloroplast biogenesis throughout development, although *atHSP93-V* seems to be relatively more important later on, most likely due to reduced expression of *atHSP93-III* at this time. Two lines of evidence confirm that the observed phenotypes were due to the presence of the *tic110*, *tic40* and *hsp93-V* T-DNA insertions. First of all, the additional alleles of each mutation described earlier (Figure 2a) exhibited identical phenotypes (Table 1, Figure 4c; data not shown). Secondly, analyses of at least 30 independent families, for each mutant, confirmed the tight genetic linkage of each visible phenotype with the corresponding T-DNA-associated selectable marker (data not shown).

Chloroplasts in the mutants have structural defects

We next addressed the question of whether the visible phenotypes of the mutants correlate with structural defects at the leaf, cellular and organellar levels. To this end, we used both light and electron microscopy to study the mutants. For *tic40* and *hsp93-V*, we analysed cotyledons from 5-day-old plants; plants of this age were used because previous work revealed more pronounced defects in young *ppi1* plants (Jarvis *et al.*, 1998). This early period of development is also characterized by high levels of plastid and cell division. Once again, the *ppi1* mutant was used as a control. Because *tic110* plants display a more severe visible phenotype in older, expanding tissues, we examined the primary leaves of 10-day-old plants for this mutant. Equivalent tissues from wild-type plants of the same age were analysed in each case.

Our light micrographs suggested that the *tic40* chloroplasts were only slightly smaller than those in the wild type (Figure 5a), but revealed that the *tic40* mesophyll cells contained significantly fewer chloroplasts than equivalent wild-type, *tic110* and *hsp93-V* cells (Figure 5a, Table 3, data not shown). By contrast, the *ppi1* mutant (which has a very similar visible phenotype to *tic40*; see Figure 4a) seemed to have much smaller chloroplasts than the wild type (Figure 5a), and a more normal number of chloroplasts per cell (Figure 5a, Table 3). Whereas the chloroplasts in *tic40* were rather sporadically distributed within each cell, *ppi1* chloroplast distribution was completely normal (Figure 5a). These differences between *tic40* and *ppi1* (as well as the ultrastructural differences referred to below) might reflect the fact that *tic40* exerts a general effect on chloroplast import (see later), whereas the *ppi1* mutation affects the import of photosynthetic proteins with a degree of specificity (Kubis *et al.*, 2003).

We also observed that the cellular organization of the mesophyll tissue was rather disorganized in both *tic40* and *ppi1* (Figure 5a). Leaf anatomy in the other, less severely pale mutants was essentially normal (data not shown), and so this phenotype is most likely a general reflection of the severity of the chloroplast biogenesis defects in these two mutants. Similar mesophyll disorganization in other chlorotic mutants has been interpreted to occur as a result of retarded growth and division rates of mesophyll cells as epidermal and vascular tissues expand (López-Juez *et al.*, 1998).

The electron micrographs revealed that wild-type chloroplasts were not completely mature at 5 days after germination, but that they nevertheless contained thylakoids and substantial granal stacks (Figure 5b). Interestingly, *tic40* chloroplasts were more spherical in shape than wild-type chloroplasts, having a rather 'swollen' appearance (Figure 5b, Table 3), and contained dramatically reduced thylakoid membrane networks with smaller granal stacks (Figure 5b); similar observations were reported by Chou *et al.* (2003). Thylakoid development was also strongly affected by the *ppi1* mutation (Figure 5b), but *ppi1* chloroplasts retained a normal, disc-like shape (Figure 5b, Table 3). The electron micrographs also confirmed the organellar size differences suggested by the light micrographs: using cross-sectional area as a measure of size, *ppi1* chloroplasts were found to be 71% smaller than wild-type chloroplasts, whereas *tic40* chloroplasts were only 45% smaller (Table 3). Finally, the *hsp93-V* and *tic110* mutant chloroplasts were less well developed than wild-type chloroplasts, but more advanced than those in *tic40* plants (Figure 5b). In all mutants, starch granule formation was delayed in comparison with wild type (Figure 5b).

Overall, the chloroplast ultrastructural phenotypes reflected the visible phenotypes of the mutants, with respect to severity, in that the most dramatic changes were observed in *tic40* (and *ppi1*) and the most mild changes were observed in heterozygous *tic110* plants. The data demonstrate that atTic110, atTic40 and atHsp93-V are required for normal chloroplast development *in vivo*. It is likely that the mutant chloroplasts do not support sufficient import of essential proteins to allow normal chlorophyll accumulation, thylakoid membrane development and chloroplast growth.

Protein import into mutant chloroplasts is defective

To obtain direct evidence that the mutations affect chloroplast protein import, the protein import efficiencies of

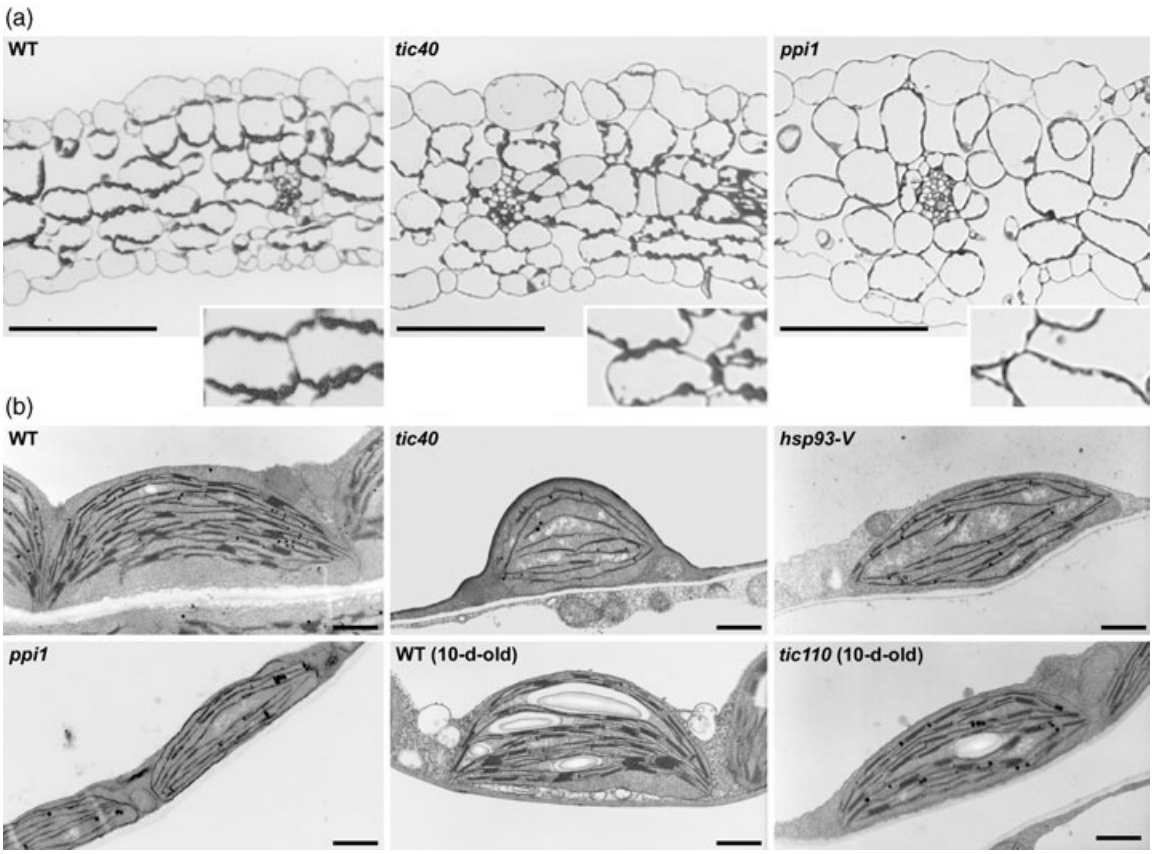

Figure 5. Light and electron microscopic analysis of the knockout mutants.
(a) Chloroplast size and distribution and leaf architecture in the knockout mutants was analysed using light microscopy. The cotyledons of 5-day-old, *in vitro*-grown plants were analysed, and representative images are shown; bars represent 100 μm. Each inset shows a twofold magnification of a part of the corresponding full-size image. The insets illustrate differences between the genotypes that are described in the text.
(b) Chloroplasts within the cotyledons of 5-day-old, *in vitro*-grown wild-type, *tic40, hsp93-V* and *ppi1* plants, or within the primary leaves of 10-day-old, soil-grown wild-type and *tic110* plants, as indicated, were analysed by transmission electron microscopy. Representative chloroplasts are shown in each case. Bars represent 1 μm.

Table 3 Quantitative analyses of light and electron micrographs

Genotype	No. chloroplasts/cell cross section ($n = 70$)	Chloroplast length (μm) ($n = 50$)	Chloroplast width (μm) ($n = 50$)	Chloroplast cross-sectional area[a] (μm^2) ($n = 50$)	Chloroplast shape (length/width) ($n = 50$)
WT	14.1 ± 3.0	6.4 ± 2.0	2.4 ± 0.7	12.4 ± 6.3	2.8 ± 0.8
tic40	7.5 ± 3.3	3.8 ± 1.0	2.3 ± 0.5	6.8 ± 2.5	1.7 ± 0.5
ppi1	14.1 ± 3.9	3.7 ± 0.8	1.2 ± 0.3	3.6 ± 1.2	3.1 ± 0.8

[a]Cross-sectional area was calculated using the following formula: $\pi \times 0.25 \times$ length $\times$ width. Thus, the values given are approximations only, as the formula calculates the area of a perfect elliptical shape.
Number of chloroplasts per cell cross-section data were calculated using light micrographs. All other data were calculated using electron micrographs.

isolated mutant chloroplasts were assessed *in vitro*. For these studies, we used the precursor of the small subunit of Rubisco (preSSU; a component of photosynthetic dark reactions) and the precursor of a 50S ribosomal subunit protein (preL11; a component of the chloroplast's endogenous genetic system). These two preproteins (one photosynthetic, one non-photosynthetic) were selected as previous studies revealed that some translocon mutations (such as *ppi1*) affect the import of photosynthetic and non-photosynthetic preproteins to different degrees (Bauer *et al.*, 2000; Ivanova *et al.*, 2004; Kubis *et al.*, 2003, 2004). The assays were carried out using established procedures (Aronsson and Jarvis, 2002; Kubis *et al.*, 2003), and thermolysin treatments confirmed the chloroplast location of the

processed protein form in each case (data not shown). Possible indirect effects of the mutations (due to photosynthetic energy deficit) were eliminated by supplementing each assay with 5 mM ATP, which is sufficient to support import in the dark to the same level as it occurs in the light (Aronsson and Jarvis, 2002).

As shown in Figure 6, import of the two tested preproteins was reduced, roughly equivalently, in all three mutants. The amount of protein imported into mutant chloroplasts, at each time point, was expressed as a percentage of the amount imported into wild-type chloroplasts by the last time point of each experiment (Figure 6). Low yields in *tic40* chloroplast isolation experiments, presumably caused by the apparent low number of chloroplasts per unit leaf area in *tic40* (Figure 5a, Table 3), limited the number of time points for which we could generate sufficient data for this mutant. The maximal amount of imported SSU was reduced by approximately 30% in *hsp93-V* chloroplasts (Figure 6a), and by approximately 40% in *tic40* chloroplasts (Figure 6e); the SSU import data reported here for *tic40* are quantitatively similar to those reported by Chou *et al.* (2003). The maximal amount of imported L11 was reduced by approximately 35% in both *hsp93-V* and *tic40* chloroplasts (Figure 6b,f). The import defect of heterozygous *tic110* chloroplasts was less pronounced. Nevertheless, small and roughly equivalent reductions in the amount of imported SSU and L11 were consistently and reproducibly observed, revealing a subtle but significant import defect (Figure 6c,d). The moderate nature of the *tic110* import defect is consistent with the moderate visible (Figure 4a) and chloroplast biogenesis (Figure 5b) defects displayed by this mutant, particularly during early development (Figure 4b).

In summary, the results show that chloroplasts from all three mutants have a reduced capacity to import proteins.

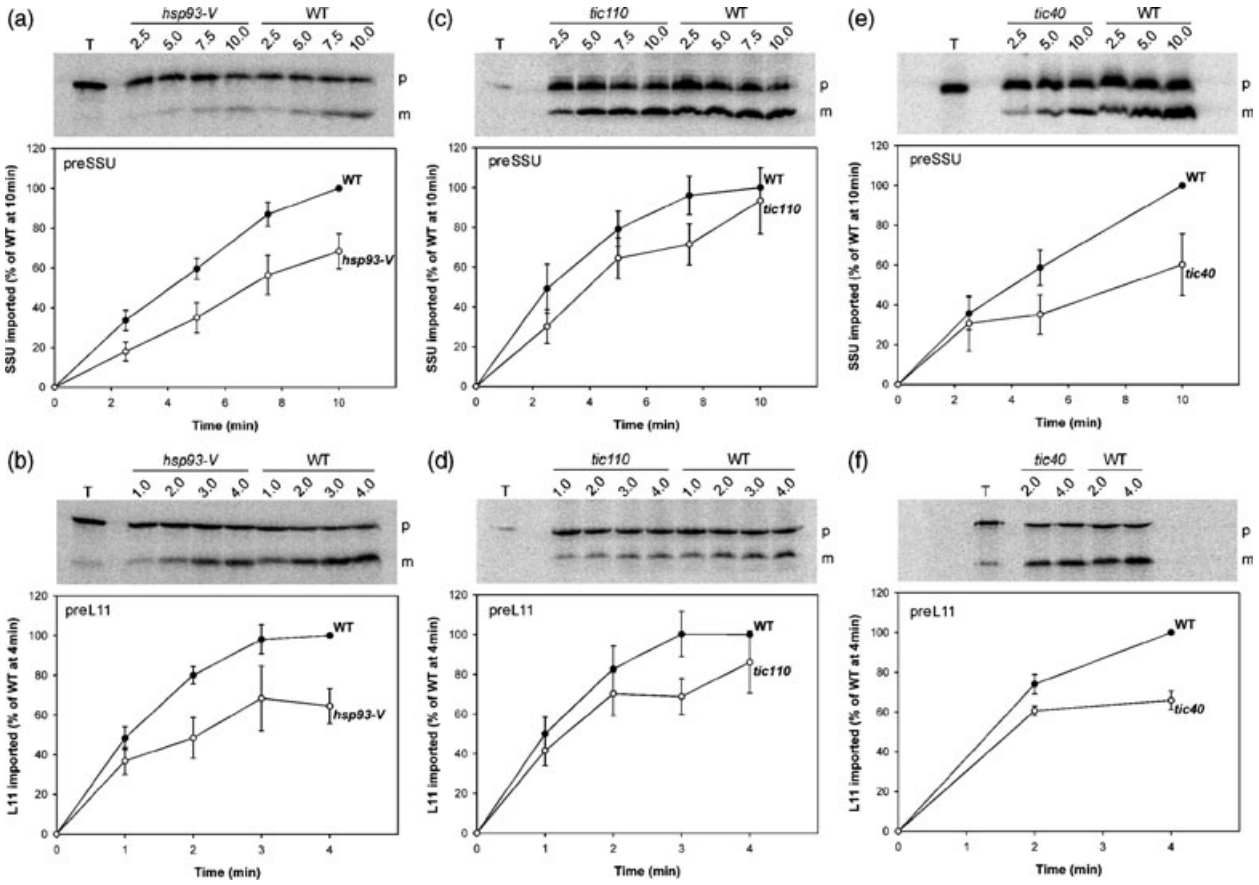

Figure 6. Protein import into knockout mutant chloroplasts is defective.
Isolated wild-type and mutant (*hsp93-V*, *tic110* or *tic40*, as indicated) chloroplasts were incubated with *in vitro*-translated, [^{35}S]methionine-labelled preSSU (a, c, e) or preL11 (b, d, f) in the presence of 5 mM ATP for the times indicated above each gel image (in minutes) and in each graph. Import reactions were analysed by SDS-PAGE, visualized using a phosphor-imager, and quantified using ImageQuant (Molecular Dynamics). Each graph shows the amount of protein imported into chloroplasts expressed as a percentage of the amount imported into wild-type chloroplasts by the last time point of each experiment. Data shown are means (± SE) derived from four (a, d, e) or three (b, c, f) independent experiments. Representative gel images are shown above each graph. T, translation product; p, precursor; m, mature. The second, shorter preL11 translation product observed in (b) and (f) corresponds to translation initiation at an ATG codon near the transit peptide-processing site.

The observed import defects were not specific to photosynthetic or non-photosynthetic preproteins, and so the data are consistent with the hypothesis that each component plays a general, non-substrate-specific role in chloroplast protein import.

Genetic interactions between the knockout mutations

To genetically assess functional relationships between the atTic110, atTic40 and atHsp93-V proteins, we crossed the corresponding knockout mutants to each other and then identified all three double-mutant combinations in subsequent generations by growth on appropriate selective media and PCR analysis. Assessment of double-mutant phenotypes is an approach commonly used to categorize and assign different mutations (and therefore genes and proteins) to different pathways and processes. Two mutations that affect different processes generally give rise to a double-mutant phenotype equal to the sum of the constituent single mutant phenotypes; this phenomenon is termed additivity. For example, double mutants possessing unrelated mutations that each affect chloroplast biogenesis have chlorotic phenotypes more severe than either single mutant (López-Juez *et al.*, 1998). By contrast, non-additive interactions – such as epistasis, in which one mutation masks the phenotype of the other – are frequently taken as evidence for a close functional relationship between the affected components.

Interestingly, when we assessed the phenotypes of our three double mutants, none were found to show phenotypic additivity (Figure 7; data not shown). Although the *hsp93-V* and *tic40* single mutants both displayed strong chlorophyll deficiencies after 10 days growth (46 and 77%, respectively, relative to wild type), *tic40 hsp93-V* double homozygotes were no more chlorotic than the *tic40* single mutant (Figure 7a). In fact, the *hsp93-V* mutation actually gave rise

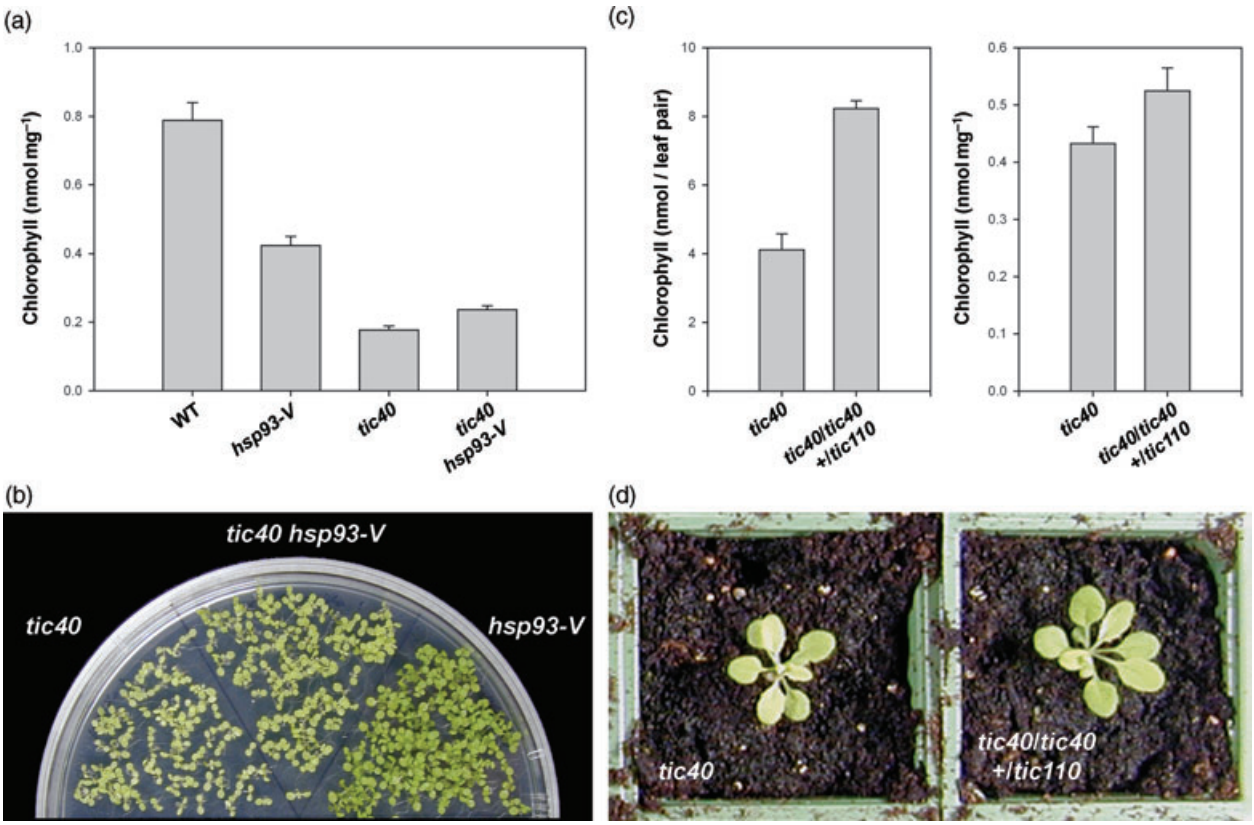

Figure 7. Genetic interactions between the knockout mutations.
(a, b) Partial suppression of the *tic40* chlorotic phenotype in *tic40 hsp93-V* double mutants. (a) Chlorophyll concentrations in 10-day-old, *in vitro*-grown plants of the indicated genotypes were determined photometrically. Values shown are means (± SD) derived from four replicates, and indicate the amount of chlorophyll per mg fresh weight of tissue. (b) Representative image of 10-day-old, *in vitro*-grown *tic40* and *hsp93-V* single-mutant plants grown alongside *tic40 hsp93-V* double-mutant plants.
(c, d) Partial suppression of the *tic40* phenotype in *tic40 tic110* (genotype: *tic40*/*tic40*; +/*tic110*) double mutants. (c) Chlorophyll in 27-day-old plants of the indicated genotypes was determined photometrically. Values shown are means (± SD) derived from five or six replicates, and indicate either the amount of chlorophyll per pair of young leaves (the fifth and sixth true leaves from each genotype were employed) (left bar chart), or the amount of chlorophyll per mg fresh weight of tissue (right bar chart); the two bar charts show the same data, expressed in slightly different ways. (d) Representative plants of the indicated genotypes were transplanted to soil from appropriate selective media after 13 days growth, and then grown for a further 10 days in a growth cabinet.

to a partial suppression of the *tic40* phenotype at this stage of development, as the double homozygote contained approximately 33% more chlorophyll than the *tic40* single mutant (Figure 7a). The double mutants were also visibly greener than *tic40* and slightly larger in size (Figure 7b). These observations were made in repeated experiments using multiple, different seed stocks for each genotype, indicating that the differences observed were not attributable to differences in seed quality. As shown in Figure 7(c,d), the *tic40* mutation could also be partially suppressed by the *tic110* mutation, as double mutants (genotype: *tic40*/*tic40*; +/*tic110*) were slightly larger and greener than *tic40* single mutants. While the *tic110* mutation did not significantly suppress the *hsp93-V* mutation, neither did it add to the *hsp93-V* phenotype, as *hsp93-V tic110* double mutants had exactly the same appearance as *hsp93-V* single mutants (data not shown).

As phenotypic additivity was not observed in any of the three double-mutant combinations examined, these data suggest that Tic110, Tic40 and Hsp93 may function in close association with each other during chloroplast protein import *in vivo*, as has been proposed based on *in vitro* biochemical data.

Discussion

We wished to gain insight into the *in vivo* roles of two inner envelope membrane proteins, atTic110 and atTic40, and a stromal Hsp100 chaperone, atHsp93-V, that have been proposed to function together during protein import into chloroplasts (Akita *et al.*, 1997; Chou *et al.*, 2003; Inaba *et al.*, 2003; Nielsen *et al.*, 1997). Therefore, we conducted a detailed, comparative study of Arabidopsis T-DNA knockout mutants lacking each component (Figure 2). The *tic110* mutation was lethal in the homozygous state (Figure 3), but heterozygotes had a visible yellow-green phenotype, as did *tic40* and *hsp93-V* homozygotes (Figure 4a). The severity of these chlorotic phenotypes (*tic40* > *hsp93-V* > *tic110*) correlated proportionally with reductions in chlorophyll accumulation (Figure 4b) and chloroplast ultrastructural defects (Figure 5).

To directly address the question of involvement of the three proteins in protein import, we analysed the import of two preproteins, preSSU and preL11, into isolated mutant chloroplasts (Figure 6). We used two different precursors in order to test the possibility that the Tic/Hsp93 proteins might operate in import pathways with distinct substrate specificities: previous studies on knockout mutants lacking preprotein receptors suggested that separate import pathways exist for photosynthetic and non-photosynthetic preproteins (Bauer *et al.*, 2000; Ivanova *et al.*, 2004; Kubis *et al.*, 2003, 2004). While the import defects of the mutants were, by and large, proportional to the severity of the corresponding visible, chlorophyll and ultrastructural defects, none of the mutations affected one preprotein significantly more than the other (Figure 6). The results are therefore consistent with the proposed roles of the proteins as general components of the import apparatus. We conclude that these three proteins mediate the import of all proteins arriving at the inner envelope membrane, in a non-selective fashion, and that they do not associate preferentially with a particular type of Toc complex (Bauer *et al.*, 2000; Ivanova *et al.*, 2004; Kubis *et al.*, 2003, 2004). The fact that the genes encoding these three proteins are expressed relatively uniformly in both photosynthetic and non-photosynthetic tissues (Figure 1) – unlike putative substrate-specific components such as atToc33 (Kubis *et al.*, 2003) – is consistent with this conclusion.

Independently, another group recently reported the identification and characterization of Arabidopsis Tic40 knockout mutants (Chou *et al.*, 2003). The results presented by Chou *et al.* (2003) are entirely consistent with the data presented here. *In vivo* accumulation of unprocessed preproteins was observed in *tic40* plants, and it was reported that the *tic40* import defect occurs at the level of inner envelope translocation, as would be expected (Chou *et al.*, 2003). One particularly interesting observation was that *tic40* chloroplasts release significant amounts of previously bound preSSU (and even mature SSU) into the medium in import assays *in vitro* (Chou *et al.*, 2003). This observation suggests that atTic40 normally functions to prevent retrograde preprotein movement, which is consistent with its proposed role in the import motor.

Although the results presented here and previously (Akita *et al.*, 1997; Chou *et al.*, 2003; Nielsen *et al.*, 1997) demonstrate that Hsp93 plays an important role in protein import, in association with the Tic complex, the data do not preclude the possibility that Hsp93 (ClpC) proteins also participate in other processes, such as protein degradation or disaggregation, when detached from the Tic and present in the stroma. Certainly, other studies have indicated that this may be the case (Shanklin *et al.*, 1995; Sokolenko *et al.*, 1998). We do not believe, however, that the two Arabidopsis Hsp93 isoforms are specialized for one or the other function, as four lines of evidence suggest that the proteins are highly redundant: (i) they share 91% amino acid sequence identity; (ii) atHsp93-III knockout plants have no obvious visible phenotypes (S. Kovacheva, J. Bédard and P. Jarvis, unpublished observation); (iii) double mutants deficient in both atHsp93-V and atHsp93-III have a much stronger chlorotic phenotype than *hsp93-V* single mutants (S. Kovacheva, J. Bédard and P. Jarvis, unpublished observation); (iv) transgenic overexpression of an *atHSP93-III* cDNA can complement the *hsp93-V* chlorotic phenotype (S. Kovacheva, J. Bédard and P. Jarvis, unpublished observation).

Previously reported biochemical studies suggested that Tic40, Tic110 and Hsp93 cooperate closely during chloroplast protein import (Akita *et al.*, 1997; Chou *et al.*, 2003;

Inaba *et al.*, 2003; Nielsen *et al.*, 1997; Stahl *et al.*, 1999). Here we describe non-additive interactions amongst the corresponding knockout mutations in double mutants, suggesting that the proteins may function together *in vivo*. Interestingly, we also observed partial suppression of the *tic40* mutant phenotype by both the *hsp93-V* mutation and the *tic110* mutation (Figure 7). As *hsp93-V* affects just one of two redundant genes, and *tic110* exists only in the heterozygous state in plants, both mutations can be regarded as dosage modulators. Stoichiometric balance between the components of a complex is thought to be important for maintaining complex functionality, and any deviations from the balanced state (through selective increases or decreases in the abundance of a particular component) can reduce the performance of the complex (Papp *et al.*, 2003). Thus, if removal of atTic40 somehow creates an imbalance within the Tic complex, it is possible that balance might be partially restored by reducing the abundance of Hsp93 or atTic110.

The semi-dominance of the *tic110* mutation is unusual, as other known translocon mutations (e.g. *ppi1*, *ppi2*, *tic40* and *hsp93-V*) are completely recessive (Bauer *et al.*, 2000; Chou *et al.*, 2003; Jarvis *et al.*, 1998; this study). This feature of the mutation most likely reflects the fact that Tic110 plays a central and essential role in the import mechanism (as evidenced by the lethality of the mutation in the homozygous state), and yet is encoded by a single gene in Arabidopsis (cf. Toc34 and Toc159). Interestingly, Tic40 is also encoded by a single gene in Arabidopsis, but *tic40* mutations are recessive and do not cause lethality in the homozygous state. This indicates that Tic40 plays a non-essential, accessory role during chloroplast protein import. A co-chaperone that regulates or optimizes the activity of a chaperone component of the import motor might fulfil these criteria.

The lethality of *tic110* demonstrates that the processes of plastid biogenesis and embryo development are tightly linked. Plastids have critical functions during early embryogenesis and seed germination, which can be attributed to their unique role as a place for the biosynthesis of essential metabolites like amino acids, fatty acids and nucleic acids, and the storage of starch as an energy source. During late embryo development, the chloroplasts also provide photosynthetic nourishment for the embryo. Several reports have demonstrated that mutations in genes of plastid function can lead to defects in embryogenesis. For instance, embryo development was arrested between the globular and heart stages when plastidic glycyl-tRNA synthetase was inactivated (Uwer *et al.*, 1998), and was defective after the heart stage when chaperonin-60α was inactivated (Apuya *et al.*, 2001). Further support for the important role of the plastid during embryogenesis was derived from studies on the *raspberry3* mutant, which is defective in a novel protein with predicted plastid localization (Apuya *et al.*, 2002).

The embryo-proper phenotype of *tic110* embryos (Figure 3i) strongly resembles those of the *raspberry* mutants (Apuya *et al.*, 2002; Yadegari *et al.*, 1994). In fact, the appearance of 'raspberry-like' protuberances on the surface of globular stage embryos is a characteristic of many mutants that arrest during early embryogenesis (Yadegari *et al.*, 1994). Similar protuberances are also present on late-maturation stage wild-type embryos, and so they are thought to be indicative of the cellular differentiation and maturation that normally occurs during late embryo development (Yadegari *et al.*, 1994). Thus, in mutants like *tic110*, it seems that cellular maturation becomes uncoupled from embryo growth and morphogenesis. Because *tic110* embryos show abnormalities well before the globular stage (the stage at which chlorophyll accumulation normally begins), it is likely that atTic110 operates during the earliest stages of plastid formation, even before chloroplast biogenesis has commenced. This observation is consistent with the notion that atTic110 is a general component of the import apparatus, and that it is not just required for the biogenesis of photosynthetic plastids.

Like atTic110, many core components of the preprotein translocase of the inner mitochondrial membrane are essential for cell viability (Pfanner *et al.*, 1997). These essential subunits include Tim44 (the membrane attachment site for mtHsp70), mtHsp70 (the chaperone which drives preprotein translocation), Mge1 (a nucleotide exchange factor, or co-chaperone, for mtHsp70) and Tim14 (a co-chaperone which stimulates ATP hydrolysis by mtHsp70) (Mokranjac *et al.*, 2003; Neupert and Brunner, 2002; Pfanner *et al.*, 1997). Thus, the fact that the *tic110* mutation is embryo-lethal is entirely consistent with the proposed role of Tic110 in chaperone recruitment (Inaba *et al.*, 2003; Nielsen *et al.*, 1997). The relatively mild phenotype associated with the *hsp93-V* mutation can be explained by the existence of a second, closely related Hsp93 gene in Arabidopsis (*atHSP93-III*), and so our data are not inconsistent with the hypothesis that Hsp93 is also a component of the putative import motor. By contrast, if Tic40 is indeed a co-chaperone component of the import motor, the fact that the *tic40* mutation is not lethal is somewhat surprising. One possible explanation for this is that the chaperone normally regulated by Tic40 is able to function at a reasonable level in the absence of its co-chaperone (unlike mtHsp70). Although Hip/Hop-type co-chaperones (to which Tic40 is related) were originally identified based on their functional association with Hsp70 and Hsp90 chaperones, it was recently reported that Sti1 (the yeast homologue of Hop) is able to interact with the Hsp100 protein, Hsp104 (the yeast homologue of ClpB), *in vitro* and *in vivo* (Abbas-Terki *et al.*, 2001). The functional significance of this interaction, however, remains to be established.

The available evidence suggests that Tic110, Tic40 and Hsp93 function together during chloroplast protein import (Akita *et al.*, 1997; Chou *et al.*, 2003; Inaba *et al.*, 2003; Nielsen *et al.*, 1997; Stahl *et al.*, 1999; this study). However, it

is clear that further work will be required before a more thorough description of the functional relationships between these proteins can be made. The knockout mutants described in this report will be useful tools for dissecting the roles and interactions of these components in the future.

Experimental procedures

Plant growth conditions

All *Arabidopsis thaliana* plants were of the Columbia-0 (Co-0) ecotype. Seeds were surface-sterilized and plants were grown on Murashige–Skoog medium as described previously (Aronsson and Jarvis, 2002). When necessary, the following antibiotics were included in the medium at the indicated concentrations: 10 μg ml^{-1} DL-phosphinothricin (Duchefa, Haarlem, The Netherlands) for *tic110-1*, *tic40-4* and *hsp93-V-1*; 15 μg ml^{-1} hygromycin B (Duchefa) for *tic40-3*; and 50 μg ml^{-1} kanamycin monosulphate (Melford Laboratories Ltd., Ipswich, UK) for *tic110-2* and *hsp93-V-2*. Addition of the demethylating agent, 5-azacytidine (50 μM; Sigma-Aldrich Company Ltd., Poole, Dorset, UK), to the medium facilitated scoring of the kanamycin-resistant phenotypes of *tic110-2* and *hsp93-V-2*. Plants grown on soil were kept in long-day photoperiods (16 h light/8 h dark).

Identification of knockout mutants

Mutant lines were obtained from the following sources: Csaba Koncz Laboratory (Ríos *et al.*, 2002), Salk Institute Genomic Analysis Laboratory (SIGnAL) (Alonso *et al.*, 2003) and Syngenta (Sessions *et al.*, 2002); the SIGnAL lines were supplied to us via the Nottingham Arabidopsis Stock Centre (NASC). The originally identified alleles were: *tic110-1* (Syngenta, line 896_D08), *tic40-3* (Csaba Koncz, line N33230), *tic40-4* (Syngenta, line 92_C10) and *hsp93-V-1* (Syngenta, line 873_G11). The subsequently identified, supportive alleles were: *tic110-2* (SIGnAL, line SALK_119667; NASC accession number, N619667) and *hsp93-V-2* (SIGnAL, line SALK_014058; NASC accession number N514058). Another group recently reported the identification of two atTic40 knockout mutants (*tic40-1* and *tic40-2*) (Chou *et al.*, 2003). The *tic40-2* allele described by Chou *et al.* (2003) was obtained from the same source as the *tic40-4* allele described here, but the locations of the respective T-DNA insertions are different: the *tic40-2* T-DNA insertion was reported to lie in exon 8, whereas the *tic40-4* insertion lies in exon 10.

The mutants were isolated according to published procedures (Alonso *et al.*, 2003; Ríos *et al.*, 2002; Sessions *et al.*, 2002); all SIGnAL mutants were identified by searching a population of sequence-indexed Arabidopsis T-DNA insertion mutants electronically at the SIGnAL website (http://signal.salk.edu). Mutant lines displaying segregation patterns consistent with the presence of a single T-DNA insertion were identified in the indicated generations (Table 1); in the case of *tic40-3*, it was necessary to make a cross to wild-type Columbia-0 before a single-insertion line could be isolated. Analyses of the progeny of at least 30 green and/or chlorotic individuals from segregating families of each mutant revealed co-segregation of the mutant phenotypes with the T-DNA-associated selectable marker in each case (data not shown), demonstrating tight genetic linkage. The genotypes of the single-insertion lines were confirmed by PCR using gene-specific and T-DNA border-specific primers (see below), and then homozygotes were generated for analysis (*tic110* homozygotes could not be identified; see Results).

The gene-specific primers used were: *tic110-1*, forward, 5′-CCCTATCTCTTTCCCCTTTTCTTCGTTCGC-3′; *tic110-1*, reverse, 5′-CTTCGTCGTCCTCGTCTTCAGTTCCATC-3′; *tic110-2*, forward, 5′-TGCAGGTCCGTAGGGTTTTCA-3′; *tic110-2*, reverse, 5′-GAGATCGGATGGGATTGTCTGG-3′; *tic40-3* and *tic40-4*, forward, 5′-GTCCTCCGGTGTTCCAAAATATCTGCCTCTG-3′; *tic40-3* and *tic40-4*, reverse, 5′-TGTATCTGTCATTCGCTTGTCCCATTCAC-3′; *hsp93-V-1*, forward, 5′-TTTTCTTCTTCGATTCGTGTTTTCTCCATT-3′; *hsp93-V-1*, reverse, 5′-ACCATTTAGCACCGTGACGTTACCTTC-3′; *hsp93-V-2*, forward, 5′-AGTGCAGTGTGGGGCGTAAAA-3′; and *hsp93-V-2*, reverse, 5′-CCGTGACTCATGAAATGTGTGC-3′. The T-DNA border-specific primers used were: *tic110-1*, *tic40-4*, *hsp93-V-1*, left border (LB), 5′-GCCTTTTCAGAAATGGATAAATAGCCTTGCTTCC-3′; *tic110-2* and *hsp93-V-2*, LB, 5′-GCGTGGACCGCTTGCTGCAACT-3′; *tic40-3*, LB, 5′-CTGGGAATGGCGAAATCAAGGCATC-3′; and *tic40-3*, right border (RB); 5′-TCAGAGCAGCCGATTGTCTGTTGTG-3′. Primer combinations which gave positive results revealed the orientation of each T-DNA insertion, as shown in Figure 2(a). All PCR products were sequenced to precisely determine the location of each T-DNA insertion.

Chlorophyll quantification

Leaf material (total aerial tissue) was collected and weighed at the time points indicated. It was shaken for 2 h in *N,N′*-dimethylformamide at room temperature in darkness, and then left overnight at 4°C for complete extraction. The absorbance of the extracted chlorophyll was recorded at 645 and 663 nm, and the total chlorophyll amount (nmol per mg fresh weight) was calculated according to Porra *et al.* (1989).

Light and electron microscopy

The analysis of cleared wild-type and *tic110* mutant embryos using Nomarski optics was performed as described previously (Goubet *et al.*, 2003). A microscope (model BHS; Olympus) equipped for differential interference contrast (model BH2-NIC; Olympus Optical Co. (UK) Ltd., London, UK) was employed for these studies.

For the studies of leaf and chloroplast structure, cotyledons from 5-day-old, plate-grown (or primary leaves from 10-day-old, soil-grown) seedlings were fixed in 2.5% (w/v) glutaraldehyde, 2% (w/v) paraformaldehyde in 0.1 M sodium cacodylate, pH 6.8, for 2 h at room temperature, and then washed several times in the same buffer. Samples were further fixed using buffered 1% (w/v) osmium tetroxide, washed three times in sterile water, and then dehydrated using an ethanol series and propylene oxide prior to infiltration with Spurr's resin. Once polymerized, both thick (0.5–1.0 μm) and thin (60–80 nm) sections were cut using a Reichert Ultracut S Microtome (Leica Microsystems (UK) Ltd., Milton Keynes, UK). The thick sections were collected on glass slides and stained using toluidine blue for light microscopy. The thin sections were collected on copper grids, stained with uranyl acetate and lead citrate using a Leica EM Stain grid stainer (Leica Microsystems (UK) Ltd.), and then viewed using a Siemens 102 transmission electron microscope (Siemens AG, Munich, Germany).

Reverse transcriptase PCR

For the expression profiles, total RNA was isolated according to Napoli *et al.* (1990), and for the verification of the knockout mutants, total RNA was isolated according to Kubis *et al.* (2003). RNA

samples (20 μg) were treated with DNAse I according to the manufacturer's instructions (DNA-*free*™; Ambion Inc., Austin, TX, USA), quantified photometrically, and then analysed on 1.3% (w/v) agarose gels containing 1.85% (v/v) formaldehyde and MOPS buffer (20 mM MOPS, 1 mM EDTA, 50 mM NaOAc, pH 7.0) to confirm concentration and quality. First-strand cDNA was synthesized using 8 μg of total RNA as template, a primer with the sequence 5′-(T)17(A/G/C)N-3′, and SuperScript II RNase H-reverse transcriptase, according to the manufacturer's instructions (Invitrogen, Carlsbad, CA, USA).

Primers specific for each gene were designed to span an intron and produce RT-PCR products of approximately 800 bp. The sequences of the primers used were: atTic110 forward, 5′-GGGAAAGCCTCGCCAGACTGAG-3′; atTic110 reverse, 5′-ATGCAAGCAAATCATTCAGCGACAAGACC-3′; atTic40 forward, 5′-CATCAACCATAGGATCACCAC-3′; atTic40 reverse, 5′-TGTATCTGTCATTCGCTTGTCCCATTCAC-3′; atHsp93-V forward, 5′-CTTGAGAAGGAGCTTAGGCAGATA-3′; atHsp93-V reverse, 5′-GATACGTCTTCCTCCTTTCTCAATCAC-3′; atHsp93-III forward, 5′-ATGAAGCTGTGCGAAGCCAAGACT-3′; atHsp93-III reverse, 5′-TTTTCGATCACGCTGCTCCCTACGTTTGA-3′; eIF4E1 forward, 5′-AAACAATGGCGGTAGAAGACACTC-3′; eIF4E1 reverse, 5′-AAGATTTGAGAGGTTTCAAGCGGTGTAAG-3′; atToc33 forward, 5′-GGTCTCTCGTTCGTGAATGG-3′; atToc33 reverse, 5′-CTGAGCGCCTATGATAAGAG-3′.

Each PCR reaction contained one-twentieth of a reverse transcription reaction. For each experiment shown in Figure 2(b), 25 cycles of amplification were used. Before conducting the experiments shown in Figure 1, the number of PCR cycles needed to produce a standard, non-saturating amount of RT-PCR product was determined for each gene; the *atHSP93-V* gene required 15 cycles and the other genes required 20 cycles of amplification. Four, independent PCR reactions for each cDNA sample were separated on agarose gels, blotted onto Hybond NX membrane (Amersham Biosciences Ltd., Little Chalfont, Bucks, UK), and hybridized with [^{32}P]-labelled gene-specific probes (the corresponding PCR product was used as a probe in each case). Hybridizations were carried out according to the manufacturer's instructions (Amersham Pharmacia). Blots were visualized using a phosphor-imager (Molecular Dynamics, Sunnyvale, CA, USA) and quantification of expression levels was performed using ImageQuant (Molecular Dynamics). Mean values for each sample were derived using the data from all four replicates. The data for the translation initiation factor, eIF4E1, were used to normalize the data for the other genes (as this gene is expressed at comparable levels in all tissue types; Rodriguez *et al.*, 1998), and the normalized values were then expressed as a percentage of the maximal value obtained for each gene (Figure 1).

Immunoblotting

Leaf material from 19-day-old, soil-grown plants was ground in liquid nitrogen and extracted with 100 μl buffer [50 mM Tris/HCl, pH 6.8, 5% (v/v) glycerol, 0.5% (w/v) SDS, 0.1% (v/v) Triton X-100, 10 mM DTT, 5 mM EDTA; 10 μl protease inhibitor cocktail (Sigma) was added per 1 ml buffer]. Insoluble material was removed by centrifugation at 20 000 ***g*** for 15 min at 4°C, and 50 μl of the extract was used for further study. Chloroplasts were isolated from 14-day-old, plate-grown plants as described previously (Aronsson and Jarvis, 2002). All protein extracts were quantified using Bradford reagent (Bio-Rad Laboratories GmbH, Munich, Germany) prior to analysis. Samples were diluted twofold in 2× SDS-PAGE sample buffer, and separated by SDS-PAGE (Laemmli, 1970). Separated proteins were stained with Coomassie brilliant blue R250 (Fisher Scientific Ltd., Loughborough, UK), or blotted onto Hybond ECL membrane (Amersham Pharmacia). Primary antibodies were polyclonal antisera raised in rabbits against pea proteins, and were kindly provided by Kenneth Cline (Hsp70), Kenneth Keegstra (Hsp93 and Tic110) and Jürgen Soll (Tic40). The secondary antibody was an anti-rabbit IgG alkaline phosphatase conjugate (Sigma), and the detection reagent was BCIP/NBT alkaline phosphatase substrate (Sigma).

Chloroplast protein import assays

Template DNA for the *in vitro* transcription/translation of preproteins (preSSU and preL11) was amplified by PCR from cDNA clones using M13 primers as described previously (Aronsson and Jarvis, 2002). Transcription/translation was performed in a coupled system containing rabbit reticulocyte lysate (TNT® T7 Quick for PCR DNA; Promega, Madison, WI, USA) or wheat germ extract (TNT® Coupled Wheat Germ Extract System; Promega), as well as [^{35}S]methionine and T7 RNA polymerase, according to the manufacturer's instructions (Promega). Identical results were obtained with the different translation systems.

Chloroplasts were isolated from 14-day-old, plate-grown plants (or occasionally from 21-day-old soil-grown plants) using described procedures (Aronsson and Jarvis, 2002; Kubis *et al.*, 2003); *tic110* chloroplasts were isolated from segregating families grown on medium containing 10 μg ml^{-1} DL-phosphinothricin. Assessments of chloroplast yield and intactness, import reactions, thermolysin treatments and quantifications were all performed according to Aronsson and Jarvis (2002). Most of the presented data were derived using plate-grown plants. One of the four preL11 *tic110* experiments, and one of the four preL11 *hsp93-V* experiments employed soil-grown plants; identical results were obtained using plate- and soil-grown plants.

Double-mutant studies

These studies were initiated by crossing *tic40-3* with *hsp93-V-1*, *tic40-3* with *tic110-1*, and *hsp93-V-1* with *tic110-1*. Phenotypic analysis and growth on appropriate selective media were used to confirm that the crosses had been successful in the F_1 generation. Segregating F_2 families were grown on appropriate selective media, and scored phenotypically, and then seedlings from each phenotypic class were transplanted to soil. It is noteworthy that the *atTIC40* and *atHSP93-V* genes are both found on chromosome 5, but separated by a distance greater than 50 cM; as expected, the knockout mutations behaved as unlinked loci in our studies. Double mutants [(*tic40*/*tic40*; *hsp93-V*/*hsp93-V*), (*tic40*/*tic40*; +/*tic110*) and (*hsp93-V*/*hsp93-V*; +/*tic110*)] were amongst the transferred F_2 plants, and their genotypes were confirmed by PCR (using primers employed during the initial mutant identifications) and by analysing their F_3 progeny on selective media.

The phenotypes of the double mutants were compared with those of the single mutants *in vitro*, until 10 days after germination, and thereafter following transplantation to soil. The *tic40 hsp93-V* double homozygote was germinated on non-selective medium for phenotypic analysis, whereas the *tic40*/*tic40*; +/*tic110* double mutant was necessarily germinated on selective medium. The *hsp93-V*/*hsp93-V*; +/*tic110* double mutant was phenotypically assessed by conducting sibling analysis (genotypes were determined by PCR) on the progeny of *hsp93-V*/*hsp93-V*; +/*tic110* plants. For all phenotypic studies, fresh seed stocks derived from plants grown in parallel were used in order to avoid any possible effects of variable seed quality.

Acknowledgements

We thank Anthony Wardle for technical assistance, and Natalie Allcock and Stefan Hyman for transmission electron microscopy. We are grateful to Kenneth Cline (Hsp70), Kenneth Keegstra (Hsp93 and Tic110) and Jürgen Soll (Tic40) for providing antibodies, and to Syngenta, SIGnAL, and NASC for providing sequence-indexed Arabidopsis T-DNA insertion mutants. Funding for the SIGnAL indexed insertion mutant collection was provided by the National Science Foundation. This work was supported by a Royal Society/North Atlantic Treaty Organization (NATO) Postdoctoral Fellowship (to S.K.), a Universities UK Overseas Research Students (ORS) Award (to J.B.), the Royal Society Rosenheim Research Fellowship (to P.J.), and Biotechnology and Biological Sciences Research Council (BBSRC) grants 91/C12976, 91/P12928 and 91/C18638 (to P.J.).

Supplementary Material

The following material is available from http://www.blackwellpublishing.com/products/journals/suppmat/TPJ/TPJ2307/TPJ2307sm.htm

Figure S1. Quantitative RNA gel blot analysis of Hsp93 gene expression.

(a) Total RNA was extracted from three independent samples of wild-type Arabidopsis seedlings grown *in vitro* and in the light for 12 days (12 d L). Five microgram aliquots of each RNA sample were subjected to RNA gel blot analysis using *atHSP93-V* and *atHSP93-III* gene-specific, [^{32}P]dCTP-labelled probes. The probes corresponded to 5′ UTR- and transit peptide-encoding regions of each gene (the only sufficiently divergent regions), and were amplified from pBluescript SK- cDNA clones (*atHSP93-V*: H8H4, accession AA042413; *atHSP93-III*: H8E3, accession AA042388) using a T7 primer (5′-TAATACGACTCACTATAGGG-3′) and the following gene-specific primers: *atHSP93-V* (5′-TTTCCCCTTGGGCACATTC-3′); *atHSP93-III* (5′-GCTTTTTCTCTCCCAGATG-3′). The probes were of similar length and contained a similar number of cytosine residues: *atHSP93-V* (341 bp, 80× C); *atHSP93-III* (321 bp, 82× C). Scintillation counting revealed that the probes did not differ in specific activity by more than 10%. All steps (including the final exposure to film) were conducted simultaneously under identical conditions. RNA extraction, probe preparation, blotting and hybridization were conducted as described by Kubis *et al.* (2003).

(b) The bands shown in (a) were quantified using Quantity One software (Bio-Rad). The values shown are means (± SD) derived from three, independent RNA samples.

References

Abbas-Terki, T., Donze, O., Briand, P.A. and Picard, D. (2001) Hsp104 interacts with Hsp90 cochaperones in respiring yeast. *Mol. Cell. Biol.* **21**, 7569–7575.

Akita, M., Nielsen, E. and Keegstra, K. (1997) Identification of protein transport complexes in the chloroplastic envelope membranes via chemical cross-linking. *J. Cell Biol.* **136**, 983–994.

Alonso, J.M., Stepanova, A.N., Leisse, T.J. *et al.* (2003) Genome-wide insertional mutagenesis of *Arabidopsis thaliana*. *Science*, **301**, 653–757.

Apuya, N.R., Yadegari, R., Fischer, R.L., Harada, J.J., Zimmerman, J.L. and Goldberg, R.B. (2001) The Arabidopsis embryo mutant *schlepperless* has a defect in the *chaperonin-60α* gene. *Plant Physiol.* **126**, 717–730.

Apuya, N.R., Yadegari, R., Fischer, R.L., Harada, J.H. and Goldberg, R.B. (2002) *RASPBERRY3* gene encodes a novel protein important for embryo development. *Plant Physiol.* **129**, 691–705.

Aronsson, H. and Jarvis, P. (2002) A simple method for isolating import-competent Arabidopsis chloroplasts. *FEBS Lett.* **529**, 215–220.

Bauer, J., Chen, K., Hiltbunner, A., Wehrli, E., Eugster, M., Schnell, D. and Kessler, F. (2000) The major protein import receptor of plastids is essential for chloroplast biogenesis. *Nature*, **403**, 203–207.

Chen, X., Smith, M.D., Fitzpatrick, L. and Schnell, D.J. (2002) In vivo analysis of the role of atTic20 in protein import into chloroplasts. *Plant Cell*, **14**, 641–654.

Chou, M.-L., Fitzpatrick, L.M., Tu, S.-L., Budziszewski, G., Potter-Lewis, S., Akita, M., Levin, J.Z., Keegstra, K. and Li, H.-m. (2003) Tic40, a membrane-anchored co-chaperone homolog in the chloroplast protein translocon. *EMBO J.* **22**, 2970–2980.

Frydman, J. and Höhfeld, J. (1997) Chaperones get in touch: the Hip-Hop connection. *Trends Biochem. Sci.* **22**, 87–92.

Goubet, F., Misrahi, A., Park, S.K., Zhang, Z., Twell, D. and Dupree, P. (2003) AtCSLA7, a cellulose synthase-like putative glycosyltransferase, is important for pollen tube growth and embryogenesis in Arabidopsis. *Plant Physiol.* **131**, 547–557.

Gutensohn, M., Schulz, B., Nicolay, P. and Flügge, U.-I. (2000) Functional analysis of the two Arabidopsis homologues of Toc34, a component of the chloroplast protein import apparatus. *Plant J.* **23**, 771–783.

Heins, L., Mehrle, A., Hemmler, R., Wagner, R., Küchler, M., Hörmann, F., Sveshnikov, D. and Soll, J. (2002) The preprotein conducting channel at the inner envelope membrane of plastids. *EMBO J.* **21**, 2616–2625.

Hinnah, S.C., Hill, K., Wagner, R., Schlicher, T. and Soll, J. (1997) Reconstitution of a chloroplast protein import channel. *EMBO J.* **16**, 7351–7360.

Hirsch, S., Muckel, E., Heemeyer, F., von Heijne, G. and Soll, J. (1994) A receptor component of the chloroplast protein translocation machinery. *Science*, **266**, 1989–1992.

Höhfeld, J., Minami, Y. and Hartl, F.-U. (1995) Hip, a novel cochaperone involved in the eukaryotic Hsc70/Hsp40 reaction cycle. *Cell*, **83**, 589–598.

Inaba, T., Li, M., Alvarez-Huerta, M., Kessler, F. and Schnell, D.J. (2003) atTic110 functions as a scaffold for coordinating the stromal events of protein import into chloroplasts. *J. Biol. Chem.* **278**, 38617–38627.

Ivanova, Y., Smith, M.D., Chen, K. and Schnell, D.J. (2004) Members of the Toc159 import receptor family represent distinct pathways for protein targeting to plastids. *Mol. Biol. Cell*, **15**, 3379–3392.

Jackson, D.T., Froehlich, J.E. and Keegstra, K. (1998) The hydrophilic domain of Tic110, an inner envelope membrane component of the chloroplastic protein translocation apparatus, faces the stromal compartment. *J. Biol. Chem.* **273**, 16583–16588.

Jackson-Constan, D. and Keegstra, K. (2001) Arabidopsis genes encoding components of the chloroplastic protein import apparatus. *Plant Physiol.* **125**, 1567–1576.

Jackson-Constan, D., Akita, M. and Keegstra, K. (2001) Molecular chaperones involved in chloroplast protein import. *Biochim. Biophys. Acta*, **1541**, 102–113.

Jarvis, P. and Soll, J. (2002) Toc, Tic and chloroplast protein import. *Biochim. Biophys. Acta*, **1590**, 177–189.

Jarvis, P., Chen, L.-J., Li, H.-m., Peto, C.A., Fankhauser, C. and Chory, J. (1998) An Arabidopsis mutant defective in the plastid general protein import apparatus. *Science*, **282**, 100–103.

Kessler, F. and Blobel, G. (1996) Interaction of the protein import and folding machineries in the chloroplast. *Proc. Natl Acad. Sci. USA*, **93**, 7684–7689.

Kessler, F., Blobel, G., Patel, H.A. and Schnell, D.J. (1994) Identification of two GTP-binding proteins in the chloroplast protein import machinery. *Science*, **266**, 1035–1039.

Ko, K., Banerjee, S., Innes, J., Taylor, D. and Ko, Z. (2004) The Tic40 translocon components exhibit preferential interactions with different forms of the Oee1 plastid protein precursor. *Funct. Plant Biol.* **31**, 285–294.

Kouranov, A., Chen, X., Fuks, B. and Schnell, D.J. (1998) Tic20 and Tic22 are new components of the protein import apparatus at the chloroplast inner envelope membrane. *J. Cell Biol.* **143**, 991–1002.

Kubis, S., Baldwin, A., Patel, R., Razzaq, A., Dupree, P., Lilley, K., Kurth, J., Leister, D. and Jarvis, P. (2003) The Arabidopsis *ppi1* mutant is specifically defective in the expression, chloroplast import and accumulation of photosynthetic proteins. *Plant Cell*, **15**, 1859–1871.

Kubis, S., Patel, R., Combe, J. *et al.* (2004) Functional specialization amongst the Arabidopsis Toc159 family of chloroplast protein import receptors. *Plant Cell*, **16**, 2059–2077.

Laemmli, U.K. (1970) Cleavage of structural proteins during the assembly of the head of bacteriophage T4. *Nature*, **227**, 680–685.

López-Juez, E., Jarvis, R.P., Takeuchi, A., Page, A.M. and Chory, J. (1998) New Arabidopsis *cue* mutants suggest a close connection between plastid and phytochrome regulation of nuclear gene expression. *Plant Physiol.* **118**, 803–815.

Lübeck, J., Soll, J., Akita, M., Nielsen, E. and Keegstra, K. (1996) Topology of IEP110, a component of the chloroplastic protein import machinery present in the inner envelope membrane. *EMBO J.* **15**, 4230–4238.

Matlack, K.E.S., Misselwitz, B., Plath, K. and Rapoport, T.A. (1999) BiP acts as a molecular ratchet during posttranslational transport of prepro-α factor across the ER membrane. *Cell*, **97**, 553–564.

Mokranjac, D., Sichting, M., Neupert, W. and Hell, K. (2003) Tim14, a novel key component of the import motor of the TIM23 protein translocase of mitochondria. *EMBO J.* **22**, 4945–4956.

Moore, T. and Keegstra, K. (1993) Characterization of a cDNA clone encoding a chloroplast-targeted Clp homologue. *Plant Mol. Biol.* **21**, 525–537.

Napoli, C., Lemieux, C. and Jorgensen, R. (1990) Introduction of a chimeric chalcone synthase gene into petunia results in reversible co-suppression of homologous genes *in trans*. *Plant Cell*, **2**, 279–289.

Neupert, W. and Brunner, M. (2002) The protein import motor of mitochondria. *Nat. Rev. Mol. Cell Biol.* **3**, 555–565.

Nielsen, E., Akita, M., Davila-Aponte, J. and Keegstra, K. (1997) Stable association of chloroplastic precursors with protein translocation complexes that contain proteins from both envelope membranes and a stromal Hsp100 molecular chaperone. *EMBO J.* **16**, 935–946.

Papp, B., Pal, C. and Hurst, L.D. (2003) Dosage sensitivity and the evolution of gene families in yeast. *Nature*, **424**, 194–197.

Perry, S.E. and Keegstra, K. (1994) Envelope membrane proteins that interact with chloroplastic precursor proteins. *Plant Cell*, **6**, 93–105.

Pfanner, N., Craig, E.A. and Hönlinger, A. (1997) Mitochondrial preprotein translocase. *Annu. Rev. Cell Dev. Biol.* **13**, 25–51.

Porra, R.J., Thompson, W.A. and Kriedemann, P.E. (1989) Determination of accurate extinction coefficients and simultaneous equations for assaying chlorophylls *a* and *b* extracted with four different solvents: verification of the concentration of chlorophyll standards by atomic absorption spectroscopy. *Biochim. Biophys. Acta*, **975**, 384–394.

Ríos, G., Lossow, A., Hertel, B. *et al.* (2002) Rapid identification of Arabidopsis insertion mutants by non-radioactive detection of T-DNA tagged genes. *Plant J.* **32**, 243–253.

Rodriguez, C.M., Freire, M.A., Camilleri, C. and Robaglia, C. (1998) The *Arabidopsis thaliana* cDNAs coding for eIF4E and eIF(iso)4E are not functionally equivalent for yeast complementation and are differentially expressed during plant development. *Plant J.* **13**, 465–473.

Schirmer, E.C., Glover, J.R., Singer, M.A. and Lindquist, S. (1996) Hsp100/Clp proteins: a common mechanism explains diverse functions. *Trends Biochem. Sci.* **21**, 289–296.

Schnell, D.J. and Hebert, D.N. (2003) Protein translocons: multifunctional mediators of protein translocation across membranes. *Cell*, **112**, 491–505.

Schnell, D.J., Kessler, F. and Blobel, G. (1994) Isolation of components of the chloroplast protein import machinery. *Science*, **266**, 1007–1012.

Seedorf, M., Waegemann, K. and Soll, J. (1995) A constituent of the chloroplast import complex represents a new type of GTP-binding protein. *Plant J.* **7**, 401–411.

Sessions, A., Burke, E., Presting, G. *et al.* (2002) A high-throughput Arabidopsis reverse genetics system. *Plant Cell*, **14**, 2985–2994.

Shanklin, J., DeWitt, N.D. and Flanagan, J.M. (1995) The stroma of higher plant plastids contain ClpP and ClpC, functional homologs of *Escherichia coli* ClpP and ClpA: an archetypal two-component ATP-dependent protease. *Plant Cell*, **7**, 1713–1722.

Sokolenko, A., Lerbs-Mache, S., Altschmied, L. and Herrmann, R.G. (1998) Clp protease complexes and their diversity in chloroplasts. *Planta*, **207**, 286–295.

Stahl, T., Glockmann, C., Soll, J. and Heins, L. (1999) Tic40, a new 'old' subunit of the chloroplast protein import translocon. *J. Biol. Chem.* **274**, 37467–37472.

Tranel, P.J., Froehlich, J., Goyal, A. and Keegstra, K. (1995) A component of the chloroplastic protein import apparatus is targeted to the outer envelope membrane via a novel pathway. *EMBO J.* **14**, 2436–2446.

Uwer, U., Willmitzer, L. and Altmann, T. (1998) Inactivation of a glycyl-tRNA synthetase leads to an arrest in plant embryo development. *Plant Cell*, **10**, 1277–1294.

Wu, C., Seibert, F.S. and Ko, K. (1994) Identification of chloroplast envelope proteins in close physical proximity to a partially translocated chimeric precursor protein. *J. Biol. Chem.* **269**, 32264–32271.

Yadegari, R., de Paiva, G.R., Laux, T., Koltunow, A.M., Apuya, N., Zimmerman, J.L., Fischer, R.L., Harada, J.J. and Goldberg, R.B. (1994) Cell differentiation and morphogenesis are uncoupled in Arabidopsis *raspberry* embryos. *Plant Cell*, **6**, 1713–1729.

Zheng, B., Halperin, T., Hruskova-Heidingsfeldova, O., Adam, Z. and Clarke, A.K. (2002) Characterization of chloroplast Clp proteins in Arabidopsis: localization, tissue specificity and stress responses. *Physiol. Plant.* **114**, 92–101.